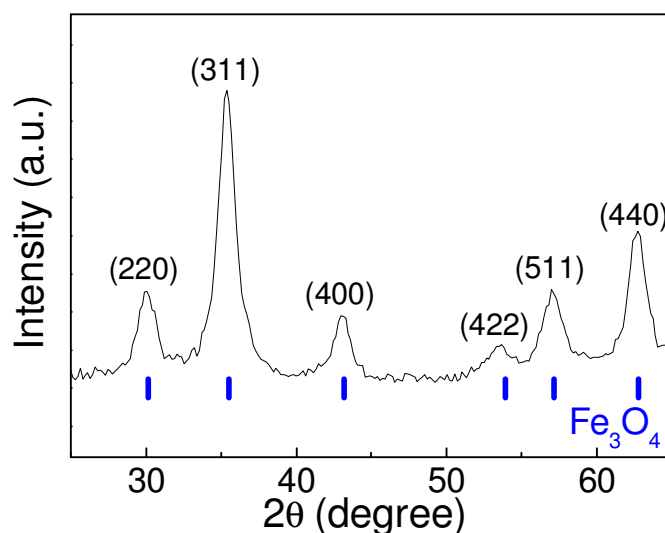


### Electronic Supplementary Information (ESI)

#### X-ray Diffraction (XRD)



**Figure S1.** XRD spectrum of sample SD, collected using a PANalytical  $\theta/\theta$  diffractometer (CuK $\alpha$  radiation; 40 kV and 40 mA). Broad peaks are visible corresponding to the spinel structure of magnetite (

#### Energy dispersive X-ray spectrometry (EDS)

Energy dispersive X-ray spectrometry (EDS) measurements are performed on the SA, SB, SC and SD samples in a Philips XL20 scanning electron microscope (SEM) equipped with a microanalysis system EDAX Phoenix (detector ECON IV). The analysis is performed on the same samples investigated by TEM, namely the TEM grids containing the NPs are mechanically attached to a home-made stub suitable to be introduced in a SEM.

A typical EDS spectrum (in particular, for sample SD), is shown in Fig. S2. The Mn and Fe signals are clearly visible and the areas under the peaks allow the software (ZAF correction) to calculate the ratio of their atomic concentration in the sample.

The atomic ratio Mn/Fe is equal to  $(0.22 \pm 0.06)$  in SD and is similar in all the samples within the errors, in good agreement with the ICP-MS results reported in the main text. The Cu signal comes from the TEM grid used to collect the NPs (the C peak, due to the carbon film on the copper grid, is observed at lower energy and therefore it does not appear in the figure).

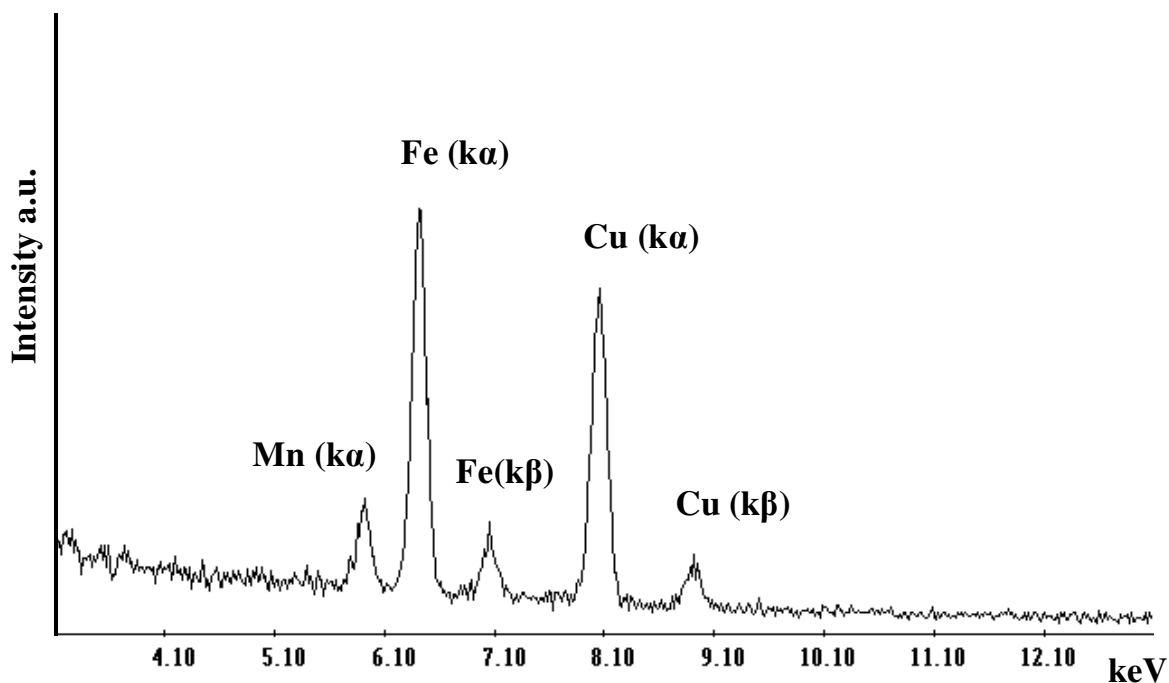


Figure S2. EDS spectrum of sample SD

#### Fourier transform infrared spectroscopy (FT-IR)

The transmission IR spectra of the NPs samples in KBr pellets are recorded on a Perkin-Elmer Spectrum 100 FT-IR spectrophotometer in the region 250–4000  $\text{cm}^{-1}$ . They appear similar for all the samples. As an example, the spectrum of sample SA is reported in Fig. S3. The bands at 1410  $\text{cm}^{-1}$ , 1543  $\text{cm}^{-1}$ , 2850–2920  $\text{cm}^{-1}$  and 3370  $\text{cm}^{-1}$  are related to the oleate; the bands at 392 and 573  $\text{cm}^{-1}$  are due to the iron-oxide phase.

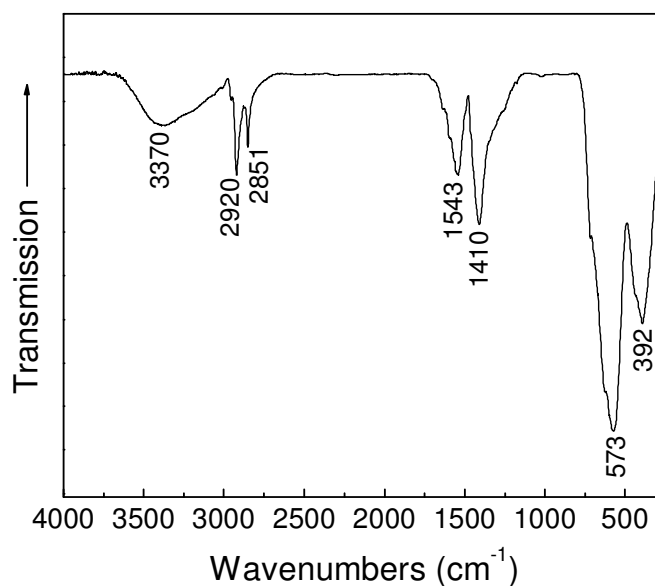
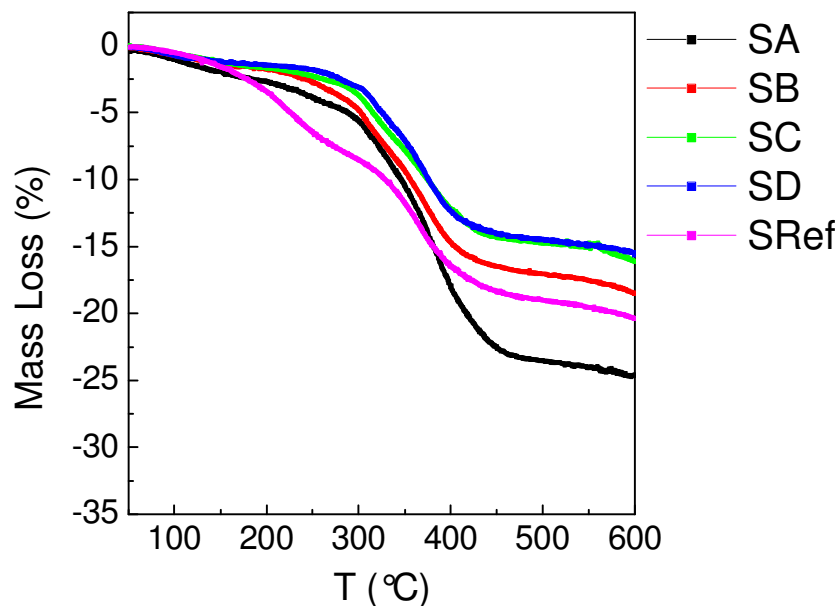


Figure S3. FT-IR spectrum of sample SA.

### Thermogravimetric analysis (TGA)



**Figure S4.** Mass loss vs. T measured in the samples of Mn-doped magnetite NPs and on the reference magnetite NPs (SRef), allowing the weight fraction of oleate in the samples to be estimated.

### SQUID measurements on samples in form of ferrofluid

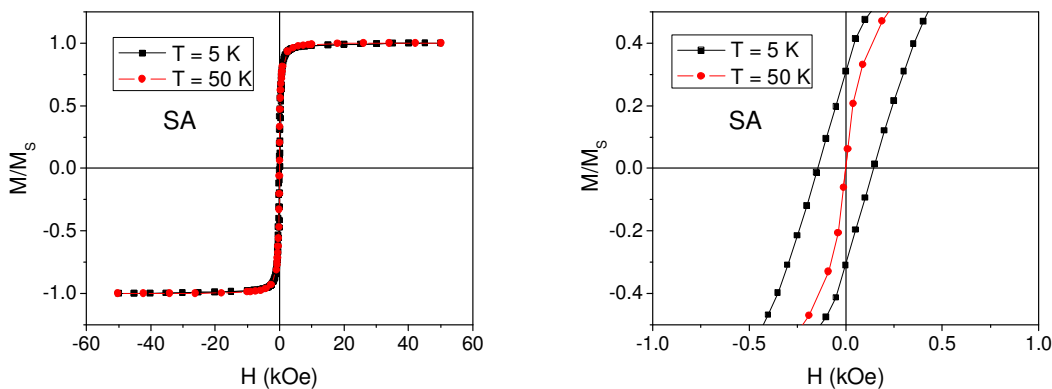


**Figure S5.** Left: magnetic hysteresis loops measured on sample SA in form of ferrofluid at T = 5 K and 50 K (normalized to the saturation magnetization  $M_S$ ). Right: enlarged view of the central region of the loops.

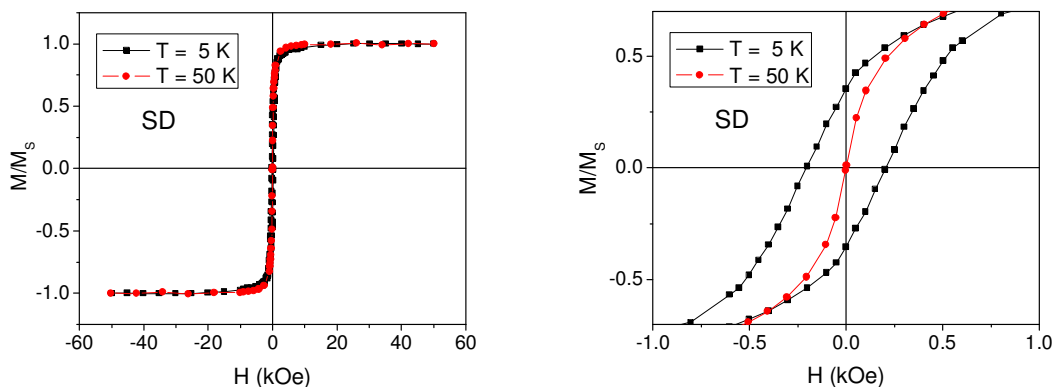


**Figure S6.** Left: magnetic hysteresis loops measured on sample SD in form of ferrofluid at  $T = 5$  K and 50 K (normalized to the saturation magnetization  $M_S$ ). Right: enlarged view of the central region of the loops.

Figs. S5 and S6 show the hysteresis loops measured on ferrofluids SA and SD, respectively. In both cases, the coercivity  $H_C$  and the remanent magnetization  $M_r$  are null at  $T = 50$  K. The same behavior is observed in the ferrofluids SB and SC.

### Dynamic Light Scattering analysis (DLS) analysis

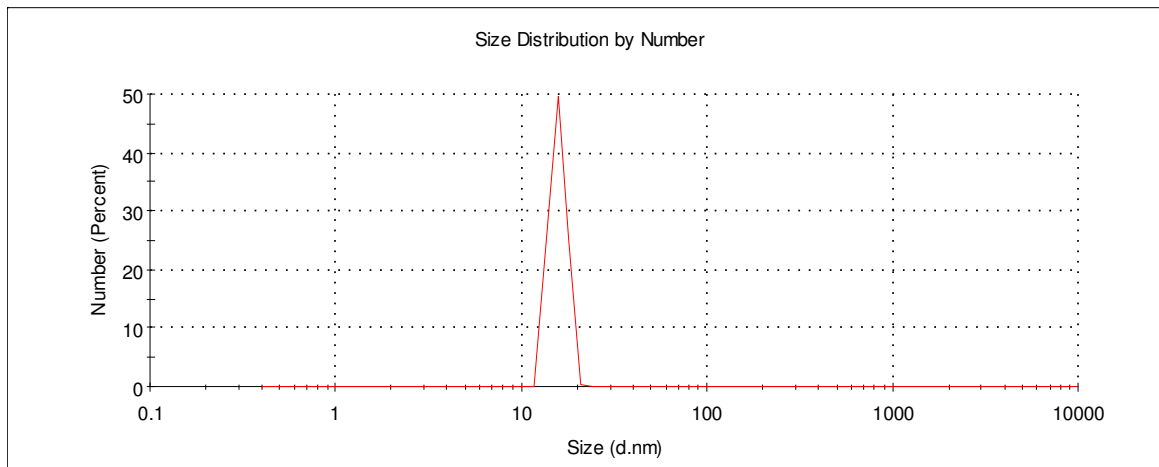


**Figure S7.** Hydrodynamic size distribution of the SB NPs measured by DLS in n-octane. The mean hydrodynamic diameter is  $(15 \pm 2)$  nm. Similar results are obtained for the other samples of Mn-doped magnetite NPs. In fact, the measured values of the mean hydrodynamic size are between 14 and 17 nm, similar for all the samples within the experimental error of 15%. These values are consistent with what is expected for oleate-coated NPs with physical size of the order of 10 nm, as in our case, dispersed in an apolar solvent [F. Arteaga-Cardona et al., *J. All. Comp.*, 2016, **663**, 636; P. de la Presa et al., *J. Phys. Chem. C*, 2015, *119*, 11022].